Available online at www.sciencedirect.com

SciVerse ScienceDirect

Ceramics International 39 (2013) 6489–6496

CERAMICS INTERNATIONAL

www.elsevier.com/locate/ceramint

Fiber/matrix interfacial shear strength of C/C composites with PyC–TaC–PyC and PyC–SiC–TaC–PyC multi-interlayers

Ying Long[a,b,c,*], Athar Javed[c,d], Yang Zhao[c], Zhao-ke Chen[b], Xiang Xiong[b], Ping Xiao[c]

[a]*School of Electromechanical Engineering, Guangdong University of Technology, No. 100 Waihuan Xi Road, Guangzhou Higher Education Mega Center, Panyu District, Guangzhou 510006, PR China*

[b]*State Key Laboratory for Powder Metallurgy, Central South University, Changsha 410083, PR China*

[c]*Materials Science Centre, School of Materials, University of Manchester, Manchester M13 9PL, UK*

[d]*Department of Physics, University of the Punjab, Quaid-i-Azam Campus, Lahore 54590, Pakistan*

Received 21 November 2012; received in revised form 14 December 2012; accepted 24 January 2013
Available online 31 January 2013

Abstract

The fiber/matrix (F/M) interfacial shear strength (IFSS) of carbon/carbon (C/C) composites with PyC–TaC–PyC and PyC–SiC–TaC–PyC multi-interlayers was investigated. To obtain C/C composites with PyC–TaC–PyC and PyC–SiC–TaC–PyC multi-interlayers, a thin layer of PyC was deposited on carbon fibers. After this, TaC and SiC–TaC layer(s) were uniformly deposited on the PyC coated carbon fibers. As an outer-layer, a PyC layer was deposited on these TaC and/or SiC–TaC coated carbon fibers by isothermal chemical vapour infiltration (CVI) and then densified with resin carbon by impregnation and carbonization. Finally, C/C composites with PyC–TaC–PyC and PyC–SiC–TaC–PyC multi-interlayers were obtained. The effects of PyC–TaC–PyC and PyC–SiC–TaC–PyC multi-interlayers on interfacial shear strength (IFSS) of C/C composites were investigated. Single fiber push-out tests were conducted on the fibers aligned perpendicularly on the thin slices specimen surface using nano-indentation. Results showed that the IFSS of C/C composites decreased with the introduction of PyC–TaC–PyC and PyC–SiC–TaC–PyC multi-interlayers. After heat treatment (at temperatures ranging from 1400 to 2500 °C) of C/C composites with PyC–TaC–PyC multi-interlayers, it was found that the IFSS decreased with the increase in temperature. This decrease in IFSS is explained by taking into account the microstructural variations on heat treatment.

Keywords: Push-out tests; PyC–TaC–PyC multi-interlayers; PyC–SiC–TaC–PyC multi-interlayers; Interfacial shear strength (IFSS)

1. Introduction

Carbon fiber-reinforced carbon (C/C) composites are of interest for aerospace and aircraft industry as structural materials due to their low density, high specific strength and low coefficient of thermal expansion (CTE) at elevated temperature [1,2]. However, the application of C/C composites is restricted due to poor oxidation resistance of carbon because it oxidizes at high temperature [3,4]. It has been reported that the oxidation resistance of composites can be improved by depositing ceramic coatings on fibers [5–9]. For example, B_4C, Si–B–C or Si–B–C/SiC multi-layer coatings on carbon fibers have been shown to protect C/C composites from oxidation remarkably well [10–12]. Furthermore, the mechanical properties of C/C composites also depend on the load transferred at the fiber/matrix (F/M) interface. Good interfacial bonding ensures the load transfer efficiently from matrix to fiber, which is helpful to reduce stress concentration and to improve overall mechanical properties [13,14]. Compressive strength and strain to failure, impact properties, fracture toughness and fatigue life are particularly sensitive to the strength of F/M interface [13]. If the interface is too weak, the fibers can be pulled out of matrix at relatively low load. On the other hand, if the interface is too strong, the brittle fracture behavior can be induced [15,16]. Thus, through proper

*Corresponding author at: School of Electromechanical Engineering, Guangdong University of Technology, No. 100 Waihuan Xi Road, Guangzhou Higher Education Mega Center, Panyu District, Guangzhou 510006, PR China. Tel.: +86 15 521139315.
E-mail address: longying0306@gmail.com (Y. Long).

0272-8842/$ - see front matter
http://dx.doi.org/10.1016/j.ceramint.2013.01.080

design of F/M interface, the oxidation resistance and mechanical properties of C/C composites can be improved effectively to enhance long term reliability of such materials from an application point of view.

In our previous study [17–19], we found that the introduction of PyC–TaC–PyC and PyC–SiC–TaC–PyC multi-interlayers had significant influence on the mechanical properties of C/C composites [17–19]. Although, the fracture mechanism, crack propagation and deflection along the F/M interface have been investigated [17–19], for better understanding, the quantitative characterization of interfacial shear strength (IFSS) at F/M interface needs to be studied. With this aim, the IFSS at the interface in C/C composites with PyC–TaC–PyC (1% and 3% TaC volume content) and PyC–SiC–TaC–PyC (5% TaC volume content) multi-interlayers is investigated for better correlation between F/M interface microstructure and mechanical behavior. The ceramic multi-layers and volume content of TaC in the composites studied here were chosen on the basis of our previous work [17–19] where it has been shown that the increase in TaC volume content to 5% and/or 10% caused a decrease in flexural strength of C/C composites with PyC–TaC–PyC multi-interlayers [18]. On the other hand, when the TaC volume content was lower than 1%, neither oxidation resistant nor mechanical properties of C/C composites could be improved significantly [19].

Up to now, several techniques, such as fragmentation tests [20,21], pull-out tests [22,23], push-out tests [3,15,24,25], push-in tests [26] and crack opening displacement [27,28] have been applied to characterize the micromechanical properties of the F/M interface in different composite systems. Among the above mentioned techniques, only the push-out tests gave a direct measure of in-situ interfacial properties. The specimens for testing were in the form of thin slices which can be cut from composites and therefore do not need/require any special manufacturing of a model material or test sample [15].

It has been demonstrated that the IFSS of C/C composites could be measured through single fiber push-out tests using nano-indentation [15] and micro-Vickers indentation [25]. An advantage of using nano-indentation technique is that it enables one carry out single fiber push-out tests on C/C composites with small fibers (~7 μm in diameter). Single fiber push-out tests consist of loading a single fiber until complete de-bonding occurs. The IFSS can be calculated through the results obtained from push-out tests. The IFSS of C/C composites obtained from normal fibers was 14.7 MPa, while for chemically strengthened fibers, the IFSS was 58.3 MPa (see Ref. [15]). Further, it is known from the literature that the measured IFSS data also depend on the type of indenter used. For example, the IFSS values reported in Ref. [25] were 37.3 MPa (measured using a spherical indenter) and 24.6 MPa measured while using a pyramidal indenter. As the fibers type, composites density and specimen thickness, used in Ref. [15] and Ref. [25] are different; a direct comparison of experimental data on IFSS between different samples could not be made [15,25].

To our knowledge, there are few reports studying the factors affecting the IFSS of C/C composites [15,25]. This may be due to problems associated with the specimen preparation, testing conditions, and/or availability of reliable modeling methods [15]. Furthermore, there is no report available in the literature studying the IFSS of C/C composites with ceramic multi-interlayers, although mechanical properties of such composites have been examined [17–19].

In the present study, single fiber push-out tests are applied to measure the IFSS (using nano-indentation) of C/C composites with and without ceramic (i.e. PyC–TaC–PyC and PyC–SiC–TaC–PyC) multi-interlayers. In addition, C/C composites with PyC–TaC–PyC multi-interlayers were heat treated from 1400 to 2500 °C to study the effect of high temperature heat treatment on IFSS.

2. Experimental procedures

2.1. Materials preparation

Needle integrated felts were used as preforms. The felts were made up of layers of non-woven long carbon fiber cloth and short-cut fiber web followed by needle-punching step by step. The carbon fiber was PAN-based (T300, 12k, Toray, Japan). The density of preforms was about 0.56 g/cm^3. A step by step preparation process of C/C composites with PyC–TaC–PyC and PyC–SiC–TaC–PyC multi-interlayers is shown in Fig. 1. A PyC layer was first deposited on carbon fibers as a buffer material using an isothermal chemical vapour infiltration (CVI) method. A gas mixture of N_2, H_2 and C_3H_6 was used at 1100 °C to deposit a PyC layer. The pressure of the gas mixture was less than 2 kPa. A SiC layer was then deposited by an isothermal CVI method using methyltrichlorosilane (CH_3SiCl_3), H_2 and Ar mixture. The SiC layer was deposited at 1100 °C with pressure less than 2 kPa and the molar ratio of H_2 to CH_3SiCl_3 was equal to 10. For the TaC layer, a $TaCl_5$–C_3H_6–Ar mixture was used. The TaC layer was deposited at a temperature of 900 °C and pressure of 600 Pa. The molar ratio of Ar:C_3H_6:$TaCl_5$ was taken as 50:3:9 respectively.

Preforms were further deposited with PyC by CVI and densified with resin carbon by impregnation and carbonization with 2–3 cycles (see Fig. 1). The impregnation and carbonization consists of three steps; (i) Furan resin impregnation in performs, (ii) solidification at 180–200 °C for 1 h and (iii) carbonization at 1000 °C for 2 h. Finally, bulk C/C composites with PyC–TaC–PyC and PyC–SiC–TaC–PyC multi-interlayers were prepared. The final relative density of prepared composites was about 88%. The C/C composites with PyC–TaC–PyC multi-interlayers were then further heat treated

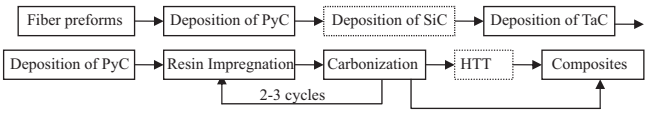

Fig. 1. Step by step preparation process of C/C composites with PyC–TaC–PyC and PyC–SiC–TaC–PyC multi-interlayers [19,32].

for 2 h (using high temperature Graphitization Induction Furnace; Model: ZGSJ-100-28) at temperatures ranging from 1400 to 2500 °C in argon atmosphere. For heating up to 1500 °C, the heating rate was set at 1000 °C/h, while for heat treatment above 1500 °C, the heating rate was 300 °C/h.

2.2. Single fiber push-out tests and interfacial shear strength (IFSS) evaluation

Single fiber push-out tests were performed by using a nano-indentation technique. A MTS Nano-indenter XP instrument with a Berkovich diamond indenter was used. A constant load at the rate of 0.2 μm/s was applied until the preset maximum load of 200 mN was reached. For single fiber push-out tests, a thin specimen is required to fracture the whole interface of the loaded fiber and to push it out completely. The prepared thin slices of thickness 88 ± 4 μm were then fixed to an aluminum holder with a groove located below the tested fibers. The groove was wide enough to facilitate the extraction of fibers while limiting the specimen bending. The specimens were then polished to obtain a smooth surface by standard metallographic procedures down to 0.25 μm by using SiC sandpaper. The well-polished specimens were dried before measuring to minimize the effects of water on the results [29].

A 40× optical microscope was used to control specimen positioning and to determine the tested fiber diameter. Each indentation was made at the center of perpendicularly aligned fibers which was identified by its perfect circular cross-section. It should be noted that due to the small fiber diameter (~7 μm), theoretically the indentation should be printed within one-third of the fiber radius (as shown in Fig. 2) during the fiber push-out tests. This ensured that the indenter did not come in contact with the matrix before de-bonding has occurred. At least 40 fibers were tested from each specimen. The surface morphologies of specimens were examined using a scanning electron microscope (SEM, Philips XL30 FEG, The Netherlands) before and after performing the push-out tests. All the data of IFSS presented in this paper were obtained from pushing out crack-free fibers (see explanation later in this paper).

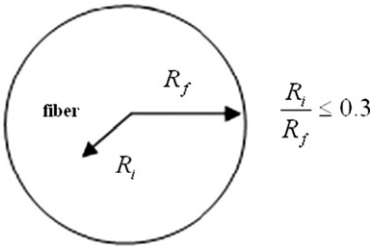

Fig. 2. Schematic of fiber radius and indentation position during single fiber push-out test.

A typical example of an indentation load–displacement curve for a single fiber push-out tests is shown in Fig. 3. At first, the indenter made inroads into the fiber (process A shown in Fig. 3(a)). As the load increases, the crack between the F/M interface initiates and propagates and the fiber deforms elastically and pushes in during process B (Fig. 3a). A flat region (process C in Fig. 3b), indicates the fiber push-out, i.e. a sudden and complete de-bonding of the interface. The indenter then touched the matrix and the load increases again during process D. In case of a sudden complete de-bonding (process C in Fig. 3(a), i.e. the flat region of the load–displacement curve in Fig. 3(b)), the IFSS can be approximated as the average shear strength of the entire interface obtained from the push-out load in load-displacement curve [24,25,30] as follows:

$$IFSS = \frac{P}{\pi\, d\, t} \tag{1}$$

where P is the push-out load, d is the fiber diameter and t is the thickness of the composites specimen.

3. Results and discussion

3.1. Microstructure analysis

Fig. 4 shows the SEM images of C/C composites with PyC–TaC–PyC and PyC–SiC–TaC–PyC multi-interlayers. From the microstructure analysis (Fig. 4 (a)), it was found

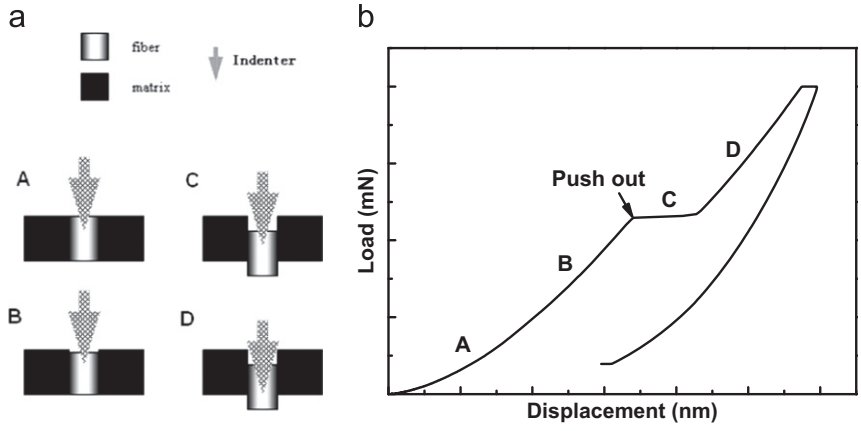

Fig. 3. (a) Schematic diagram and (b) typical indentation curve under push-out tests.

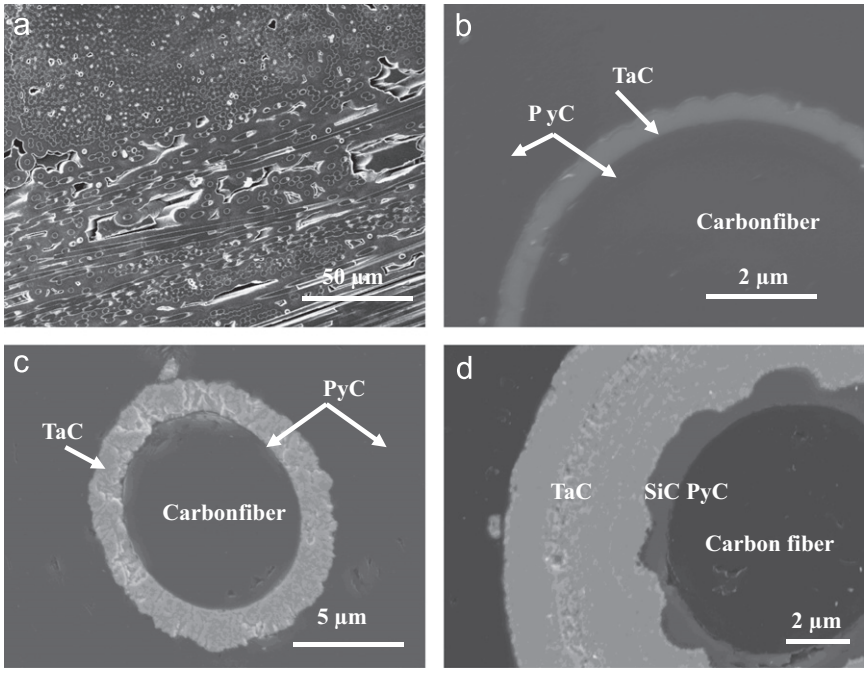

Fig. 4. SEM images of C/C composites with PyC–TaC–PyC multi-interlayers (a) an overview, (b) and (c) distribution of PyC and TaC layers with different TaC thicknesses and (d) distribution of PyC, SiC and TaC layers in C/C composites with PyC–SiC–TaC–PyC multi-interlayers.

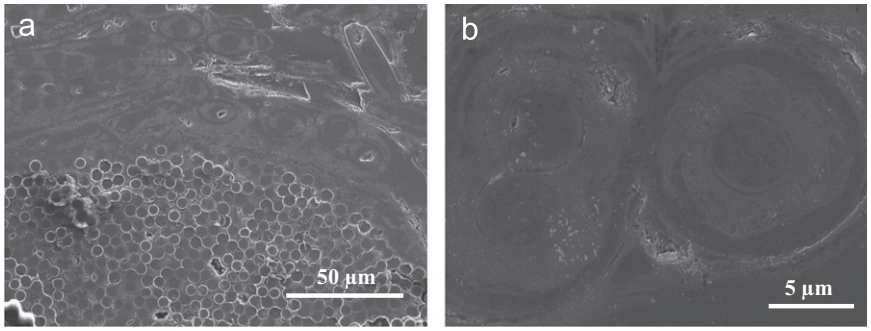

Fig. 5. (a) Polish-induced protuberant fibers and (b) de-cohesion at the F/M interface.

that the composites were mainly composed of carbon fibers, multi-interlayers, matrix, pores and cracks. The PyC–TaC–PyC multi-interlayers around carbon fibers can be seen from SEM images shown in Fig. 4(b and c). The volume content of fiber in composites is about 10% as mentioned earlier. From the SEM images shown in Fig. 4(b and c), it is difficult to see clearly the interface between the carbon fiber and PyC because both carbon fiber and PyC have black color in the SEM images. However, for fibers standing out of matrix during polishing, a clear PyC layer was observed between fiber and TaC layer (see Fig. 6(d)). The inner PyC layer with a thickness of about 0.2 μm was well aligned around the transverse fiber surface while the TaC interlayer deposited uniformly between two layers of PyC was clearly observed. It should be noted that 1% and 3% volume contents of TaC layers over the total volume of the composites were obtained by controlling deposition time during the deposition process. The thickness of TaC layer was determined by the volume content. Thus, 1% volume content of TaC interlayer in C/C composites gave a TaC thickness of about 0.3 ± 0.05 μm (Fig. 4(b)) while for 3% volume of TaC, the achieved thickness of the TaC layer was around 1.0 ± 0.2 μm (Fig. 4(c)). From the microstructure of C/C composites with PyC–SiC–TaC–PyC multi-interlayers, it was seen (Fig. 4(d)) that both inner PyC layer and SiC layer were about 0.2 ± 0.05 and 1.0 ± 0.2 μm thick respectively, while the thickness of the TaC layer was about 4.0 ± 0.5 μm.

3.2. Effect of PyC–TaC–PyC and PyC–SiC–TaC–PyC multi-interlayers on IFSS of C/C composites

To investigate the effect of PyC–TaC–PyC and PyC–SiC–TaC–PyC multi-interlayers on IFSS of C/C composites, single fiber push-out tests were first conducted on

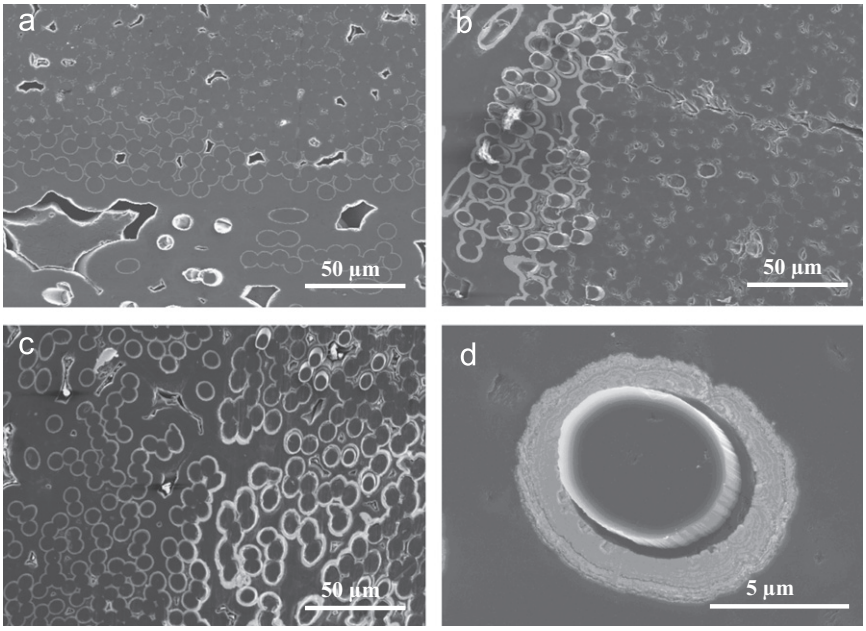

Fig. 6. SEM images of specimen surface of C/C composites with PyC–TaC–PyC multilayers after polishing (a) 0.3 μm thick TaC, (b) 1.0 μm thick TaC layer; (c) PyC–SiC–TaC–PyC and (d) close-up of protuberant fiber.

pure C/C composites as a reference. As-polished thin specimens possess protuberant fibers which stand out of the matrix after polishing as shown in Fig. 5(a). A similar result was obtained by Rollin et al. [15]. F/M interface de-cohesion was found after polishing (Fig. 5(b)). This was also observed by Desaeger and Verpoest [31]. The fiber protuberant and de-cohesion could be attributed to residual stress relaxation associated with the interface degradation during sample preparation and this suggested the presence of a weak F/M interface.

The protuberant fibers were also observed in polished C/C composites with PyC–TaC–PyC and PyC–SiC–TaC–PyC (Fig. 6). The close-up of a protuberant fiber (Fig. 6(d)) showed that the fiber with multi-interlayers failed at the fiber/PyC interface while the PyC layer was still adhered to the TaC layer. In the present work, protuberant fiber and fiber with de-cohesion interface were avoided for the nano-indentation test. Furthermore, all samples were polished under similar metallographic conditions (as motioned above) to reduce the surface roughness variation created during polishing. It should be noted that the polishing is an essential step for sample preparation.

Nano-indentation was made on a single fiber until it was separated from the matrix. SEM images of pure C/C composites taken after push-out tests (Fig. 7) confirmed the movement of carbon fiber through the matrix. After pushing out, no visible damage of fiber or matrix was found. This demonstrated that the de-bonding only occurred at the F/M interface after the push-out tests. For C/C composites with PyC–SiC–TaC–PyC multi-interlayers, the failure always occurred at the fiber/PyC interface during fiber push-out tests (see Fig. 7(b)). The push-out load (P) was obtained from the load–displacement curves and the IFSS was estimated using Eq. (1). Table 1 presents the data on push-out-load (P) and IFSS obtained from tested composites. Repeated measurements confirmed that the reproducibility of push-out tests lie within the calculated standard deviation.

From Table 1, it can be seen that the IFSS values of C/C composites decreased with the introduction of PyC–TaC–PyC and PyC–SiC–TaC–PyC multi-interlayers. It was noted that when the SiC interlayer was deposited between PyC and TaC, the IFSS of C/C composites with PyC–SiC-4 μm TaC–PyC composites was slightly higher than that of C/C composites without SiC interlayer (i.e. C/C composites with PyC–TaC–PyC multi-interlayers). However, for composites with 0.3 μm and 1 μm thick TaC interlayers, the IFSS values were almost similar within the calculated error.

It has been shown that the PyC–TaC–PyC and PyC–SiC–TaC–PyC multi-interlayer has a significant effect on fracture behavior of C/C composites [17–19]. Higher IFSS in pure C/C composites makes the composites fail in a brittle manner (Table 1). The fracture surface of pure C/C composites is thus rather flat without any fiber pull-out in the bending fracture surface [18]. With the introduction of PyC–TaC–PyC multi-interlayer, C/C composites have a lower IFSS, which allows pull-out of large amounts of fibers, fiber clusters and multi-interlayers. As a result, the composites showed pseudo-plastic fracture behavior [17–19]. When the PyC–SiC–TaC–PyC multi-interlayers were introduced into C/C composites, the fracture surface of composites became mostly flat again. However, some fiber bundles were still present parallel to the fracture surface. Furthermore, the fiber bundles perpendicular to the

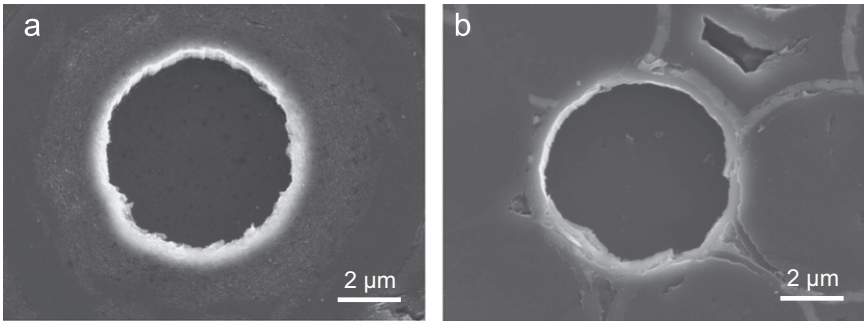

Fig. 7. SEM images taken after fiber push-out tests from fibers: (a) pure C/C composites and (b) C/C composites with PyC–TaC–PyC multi-interlayers.

Table 1
Composites total thickness t, push-out load P and calculated IFSS of C/C composites with different multi-interlayers.

Composites	t (μm)	P (mN)	IFSS (MPa)	Fracture behavior
Pure C/C	84	97 ± 7	53 ± 4	Brittle[a]
C/C–PyC-0.3 μm TaC–PyC	89	73 ± 8	37 ± 4	Pseudo-ductile[b]
C/C–PyC-1 μm TaC–PyC	85	65 ± 6	35 ± 3	Pseudo-ductile[a]
C/C–PyC–SiC-4 μm TaC–PyC	92	82 ± 7	41 ± 3	Brittle[c]

Note: C/C, C/C–PyC-0.3 μm TaC–PyC, C/C–PyC-1 μm TaC–PyC and C/C–PyC–SiC-4 μm TaC–PyC represent the C/C composites without any additional layer on carbon fiber, with PyC-0.3 μm TaC–PyC, PyC-1 μm TaC–PyC and PyC–SiC-4 μm TaC–PyC ceramic multi-interlayers on carbon fiber respectively.
[a]Ref. [19].
[b]Ref. [17].
[c]Ref. [18].

fracture surface partially pulled-out of the fiber. This was an indication of fracture toughness improvement compared to the pure C/C composites [17–19]. The improved fracture behavior could be attributed to the decrease in interface bonding strength. Smaller IFSS promoted the debonding of interface which resulted in better fracture behavior of C/C composites.

3.3. Effect of heat treatment on IFSS of C/C composites with PyC–TaC–PyC multi-interlayers

Push-out tests were also carried out on composites with heat treatments at different temperatures. Fig. 8 shows the average measured IFSS of C/C composites with PyC-0.3 μmTaC–PyC multi-interlayers as a function of heat treatment temperature. It was found that the IFSS decreased drastically with the increase in heat treatment temperature. After heat treatment at different temperatures, the change in surface morphology of C/C/ composites with PyC-0.3 μm TaC–PyC multi-interlayers was observed from SEM. Representative SEM images (taken after heat treatment at 1800 °C and 2500 °C) of C/C composites with PyC–TaC–PyC multi-interlayers are shown in Fig. 9. From the analysis of SEM images, it was found that the heat treatment led to the formation of cracks at the interfaces. Furthermore, it was found that the TaC crystallites grew on heat treatment at high temperature. Thus, the decrease in IFSS with the increase

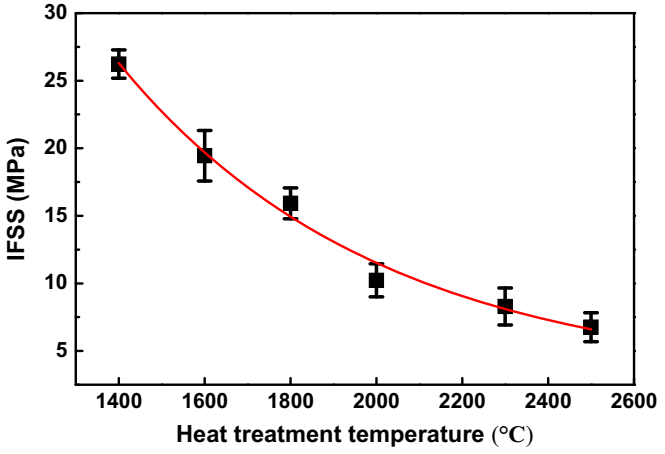

Fig. 8. IFSS of C/C composites with PyC-0.3 μm TaC–PyC multi-interlayers as a function of temperature. The red solid line is an exponential fit to the experimental data and is a guide for the eye. (For interpretation of the references to color in this figure legend, the reader is referred to the web version of this article.)

in heat treatment temperature could be explained by the following facts: (i) the formation of cracks between the interfaces (see SEM image shown in Fig. 9(a)) can lead to the decrease in IFSS; (ii) the growth of TaC crystals [18] (see SEM image in Fig. 9(b)); and (iii) serious damage of TaC coating (Fig. 9(b)) [18]. At 2500 °C, the damage of carbon fibers was observed (see Fig. 9(b)) which was caused by the grain growth of TaC coatings. In addition,

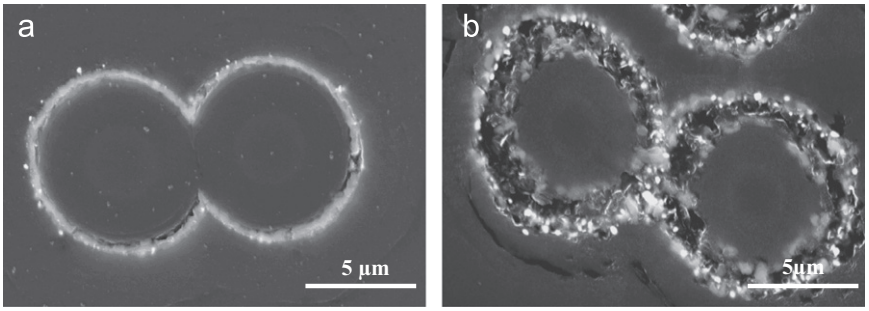

Fig. 9. SEM images showing microstructure of C/C composites with PyC–TaC–PyC multi-interlayers after heat treatment at (a) 1800 °C and (b) 2500 °C.

with the increase in heat treatment temperature, carbon atoms reorganized in PyC interlayer and in the matrix with low shear resistance. As a result, the interface becomes weaker and weaker with the increase in temperature. Thus, the evaluated interfacial shear strength decreased with the increase in temperature.

4. Conclusion

In conclusion, the effect of PyC–TaC–PyC and PyC–SiC–TaC–PyC multi-interlayers on the interfacial shear strength (IFSS) of C/C composites was studied. Single fiber push-out tests were conducted (by nano-indentation) on C/C composites with ceramic multi-interlayers. The analysis of surface morphology of the fiber/matrix (F/M) interface confirmed the movement of carbon fiber through the matrix. After push-out, no damage of fiber or matrix was found which confirmed that the de-bonding only occurred at the F/M interface after the push-out tests. It was found that the IFSS of C/C composites decreased with the introduction of PyC–TaC–PyC and PyC–SiC–TaC–PyC multi-interlayers. C/C composites with multi-interlayers had almost similar IFSS which was $\sim 14 \pm 2$ MPa lower than that of pure C/C composites. The IFSS of C/C composites with PyC-0.3 μmTaC–PyC multi-interlayers decreased from 26 ± 2 MPa to 7 ± 2 MPa with the increase in heat treatment temperature from 1400 °C to 2500 °C. On heat treatment, the cracks formed at the interfaces (between F/M and ceramic multi-interlayers), growth of TaC crystallites and damaging of TaC coating was found to cause a decrease in IFSS.

Acknowledgment

We are thankful to Paul Hawksworth at the Department of Materials Science and Engineering, University of Sheffield, UK for his support in improving/polishing the English language.

References

[1] P. Diss, J. Lamon, L. Carpentier, J.L. Loubet, P. Kapsa, Sharp indentation behaviour of carbon/carbon composites and varieties of carbon, Carbon 40 (2002) 2567–2579.

[2] A. Takuya, H. Hiroshi, H. Taku, F. Hiroshi, S. Ichiro, SiC/C multi-layered coating contributing to the antioxidation of C/C composites and the suppression of through-thickness cracks in the layer, Carbon 39 (2001) 1477–1483.

[3] E.L. Corral, R.E. Loehman, Ultra-high-temperature ceramic coatings for oxidation protection of carbon–carbon composites, Journal of Ceramic Society 91 (5) (2008) 1495–1502.

[4] Z.-K. Chen, X. Xiong, B.-Y. Huang, G.-D. Li, F. Zheng, P. Xiao, H.-B. Zhang, J. Yin, Phase composition and morphology of TaC coating on carbon fibers by chemical vapour infiltration, Thin Solid Films 516 (2008) 8248–8254.

[5] R. Naslain, The design of the fiber-matrix interfacial zone in ceramic matrix composites, Composites Part A 29A (1998) 1145–1155.

[6] R. Naslain, J. Lamon, R. Pailler, X. Bourrat, A. Guette, F. Langlais, Micro/minicomposites: a useful approch to the design and development of non-oxide CMCs, Composites: Part A 30 (1999) 537–547.

[7] G.N. Morschera, J.D. Cawley, Intermediate temperature strength degradation in SiC/SiC composites, Journal of the European Ceramic Society 22 (2002) 2777–2787.

[8] S. Bertrand, C. Droillard, R. Pailler, X. Bourrat, R. Naslain, TEM structure of $(PyC/SiC)_n$ multilayered interphases in SiC/SiC composites, Journal of the European Ceramic Society 20 (2000) 1–13.

[9] S. Pasquier, J. Lamon, R. Naslain, Tensile static fatigue of 2D SiC/SiC composites with multilayered $(PyC–SiC)_n$ interphases at high temperatures in oxidizing atmosphere, Composites Part A 29A (1998) 1157–1164.

[10] S. Labruquere, H. Blanchard, R. Pailler, R. Naslain, Enhancement of the oxidation resistance of interfacial area in C/C composites. Part I: oxidation resistance of B–C, Si–B–C and Si–C coated carbon fibres, Journal of European Ceramic Society 22 (2002) 1001–1009.

[11] S. Goujard, L. Vandenbulcke, H. Tawil, Oxidation tests of carbonaceous composite materials protected by Si–B–C CVD coatings, Thin Solid Films 245 (1994) 86–97.

[12] S. Goujard, L. Vandenbulcke, H. Tawil, Oxidation behavior of 2D and 3D carbon/carbon thermostructural materials protected by CVD polylayer coatings, Thin Solid Films 252 (1994) 120–130.

[13] A. Godara, L. Gorbatikh, G. Kalinka, A. Warrier, O. Rochez, L. Mezzo, F. Luizi, A.W. van Vuure, Interfacial shear strength of a glass fiber/epoxy bonding in composites, Composites Science and Technology. 70 (2010) 1346–1352.

[14] J. Zhang, R. Luo, Y. Zhang, Y. Ni, J. Li, C. Yang, Effect of isotropic interlayer on the mechanical and thermal properties of carbon/carbon composites, Materials Letters 64 (2010) 1536–1538.

[15] M. Rollin, S. Jouannigot, J. Lamon, R. Pailler, Characterization of fibre/matrix interfaces in carbon/carbon composites, Composites Science and Technology 69 (2009) 1442–1446.

[16] R.J. Kerans, T.A. Parthasarathy, Crack deflection in ceramic composites and fiber coating design criteria, Composites Part A 30 (1999) 521–524.

[17] B. Li and Z.K. Chen, unpublished work.

[18] X. Xiong, Y.-L. Wang, Z.-K. Chen, G.-D. Li, Mechanical properties and fracture behaviors of C/C composites with PyC/TaC/PyC, PyC/

SiC/TaC/PyC multi-interlayers, Solid State Sciences 11 (2009) 1386–1392.
[19] Z.-K. Chen, X. Xiong, G.-D. Li, Y.-L. Wang, Mechanical properties and oxidation behaviors of carbon/carbon composites with C–TaC–C multi-interlayer, Journal of Materials Science 45 (2010) 3477–3482.
[20] Y.L. Yilmaz, Analyzing single fiber fragmentation test data by using sress transfer model, Journal of Composites Materials 36 (2002) 537–551.
[21] S. Lee, T. Nguyen, J. Chin, T.J. Chuang, Analysis of the single-fiber fragmentation test, Journal of Materials Science 33 (1998) 1–8.
[22] T. Ramanathan, A. Bismarck, E. Schulz, K. Subramanian, The use of a single-fibre pull-out test to investigate the influence of acidic and basic surface groups on carbon fibers on the adhesion to poly (phenylene sulfide) and matrix-morphology-dependent fracture behavior, Composites Science and Technology 61 (2001) 1703–1710.
[23] Y.R. Zhao, Y.M. Xing, Z.K. Lei, F.C. Lang, Interfacial stress transfer behavior in a specially-shaped fiber/matrix pullout test, Acta Mechanica Sinica 26 (2010) 113–119.
[24] D.K Shetty, Shear-lag analysis of fiber push-out (indentation) tests for estimating interfacial friction stress in ceramic-matrix composites, Journal of the American Ceramic Society 71 (2) (1988) C-107–C-109.
[25] Y. Furukawa, H. Hatta, Y. Kogo, Interfacial shear strength of C/C composites, Carbon 41 (2003) 1819–1826.
[26] C.A. Lewinsohn, C.H. Henager Jr., R.H. Jones, Measuring interphase recession by fiber push-in testing, Journal of the American Ceramic Society 84 (4) (2001) 866–868.
[27] S.H. Ju, S.H. Liu, Determining stress intensity factors of composites using crack opening displacement, Composites Structures 81 (2007) 614–621.
[28] V.K. Srivatava, Prediction of crack tip opening displacement of fiber composites, Engineering Fracture Mechanics 42 (5) (1992) 869–872.
[29] K. Honda, Y. Kagawa, Analysis of shear stress distribution in pushout process of fiber-reinforced ceramics, Acta Metallurgica et Materialia 43 (4) (1995) 1477–1487.
[30] T. Hinoki, W. Zhang, A. Kohyama, S. Sato, T. Noda, Effect of fiber coating in interfacial shear strength of SiC/SiC by nano-indentation, Journal of Nuclear Materials 258–263 (1998) 1567–1571.
[31] M. Desaeger, I. Verpoest, On the use of the micro-indentation test technique to measure the interfacial shear strength of fiber-reinforced polymer composites, Composites Science and Technology 48 (1993) 215–226.
[32] Z.-K. Chen, X. Xiong, G.-D. Li, Y.-L. Wang, Ablation behaviors of carbon/carbon composites with C–SiC–TaCmulti-interlayers, Applied Surface Science 255 (2009) 9217–9223.